

# Collider searches for dark matter in events with a $Z$ boson and missing energy

Linda M. Carpenter,<sup>1,2</sup> Andrew Nelson,<sup>2</sup> Chase Shimmin,<sup>2</sup> Tim M.P. Tait,<sup>2</sup> and Daniel Whiteson<sup>2</sup>

<sup>1</sup>*Department of Physics The Ohio State University, Columbus, OH 43210*

<sup>2</sup>*Department of Physics and Astronomy, University of California, Irvine, CA 92697*

Searches for dark matter at colliders typically involve signatures with energetic initial-state radiation without visible recoil particles. Searches for mono-jet or mono-photon signatures have yielded powerful constraints on dark matter interactions with Standard Model particles. We extend this to the mono- $Z$  signature and reinterpret an ATLAS analysis of events with a  $Z$  boson and missing transverse momentum to derive constraints on dark matter interaction mass scale and nucleon cross sections in the context of effective field theories describing dark matter which interacts via heavy mediator particles with quarks or weak bosons.

PACS numbers: 95.35.+d, 14.70.Bh

The particle nature of dark matter is one of the greatest outstanding mysteries of cosmology and particle physics. A suite of dedicated experiments seek to shed light on how dark matter interacts with Standard Model (SM) particles by looking for detection of ambient dark matter either directly scattering with heavy nuclei or indirectly through its annihilation into high energy Standard Model particles. An important third pillar to the search for the particle nature of dark matter is furnished by high energy particle accelerators, which can produce pairs of dark matter particles, which are expected to manifest as an excess of events showing an imbalance in momentum conservation. Searches for missing transverse momentum are a major activity at the LHC precisely because of their potential connection to dark matter [1].

Searches for dark matter in missing momentum channels can be classified based on the visible particles against which the invisible particles recoil. Existing experimental studies have considered cases in which the visible radiation is a jet of hadrons (initiated by a quark or gluon) [2–4], a photon [5, 6], or a  $W$  boson decaying into leptons [7]. These studies are performed in the context of an effective field theory (EFT) which captures the physics of a heavy particle mediating an interaction between dark matter and quarks and/or gluons. In this article, we extend the menu of such searches to include the case of a  $Z$  boson decaying into a pair of charged leptons (electrons or muons) and recast the recent ATLAS measurement of  $ZZ \rightarrow \ell\ell\nu\nu$  [8] into a bound on production of dark matter in association with a  $Z$  boson<sup>1</sup>. Since our signature consists of a pair of leptons consistent with a  $Z$  boson decay recoiling against transverse momentum car-

ried by particles invisible to the detector, we refer to our selection as a “mono- $Z$ ” signature.

We work in the context of EFTs where the dark matter’s primary interactions are with quarks or directly with electroweak bosons. In the case where interactions are primarily with quarks, the mono- $Z$  signature arises from a  $Z$  boson which is radiated from a  $q\bar{q}$  initial state, much like mono-jets or mono-photons. Such interactions also imply (depending on the specific form of the interaction) large rates for scattering with heavy nuclei. The case of direct interactions with a pair of  $Z$  bosons is more challenging to connect to direct detection (however, see [11]), and is a particular strength of collider searches. As usual, in both cases the EFT will break down at an energy not far above the one which characterizes the strength of the interactions written as higher dimensional operators, and is only a good description of the physics for processes taking place at energies well below this cut-off scale.

## EFFECTIVE FIELD THEORY

### Interactions with Quarks

Effective field theories for dark matter interacting primarily with SM quarks have been considered in Refs. [12–21]. We consider the interactions,

$$\sum_q \left\{ \frac{m_q}{\Lambda_{D1}^3} \bar{q}q \bar{\chi}\chi + \frac{1}{\Lambda_{D8}^2} \bar{q}\gamma^\mu\gamma_5 q \bar{\chi}\gamma_\mu\gamma_5\chi + \frac{1}{\Lambda_{D5}^2} \bar{q}\gamma^\mu q \bar{\chi}\gamma_\mu\chi + \frac{1}{\Lambda_{D9}^2} \bar{q}\sigma^{\mu\nu} q \bar{\chi}\sigma_{\mu\nu}\chi \right\} \quad (1)$$

where  $\chi$  is the dark matter particle, which we assume to be a Dirac fermion,  $q$  is a SM quark, and the coefficients  $\Lambda$  parameterize the coupling strength of scalar (D1), vector (D5), axial-vector (D8), and tensor (D9) interactions between the two. The labeling scheme is adopted from Ref. [18], with the choices dictated as those operators

<sup>1</sup> This signature has previously been considered in the context of a collider search for  $Z'$  decaying to invisible modes (Ref. [9]), and more recently in the dark matter context with a slightly more model-dependent framework in Ref. [10].

which lead to a non-vanishing scattering rate with nucleons at small momentum transfer. We will typically consider one interaction type to dominate at a time, and will thus keep one  $\Lambda$  finite while the rest are sent to infinity and decoupled. These operators are normalized so as to be consistent with minimal flavor violation.

### Interactions with $Z$ Bosons

One may also construct an EFT in which the dark matter interacts directly with pairs of electroweak bosons. Given our assumption that  $\chi$  is a SM gauge singlet, all such interactions are higher dimensional operators. Such operators begin at dimension 7, though through electroweak symmetry breaking they also imply effectively dimension 5 descendant operators as well.

The dimension 5 terms originate from,

$$\frac{1}{\Lambda_5^3} \bar{\chi} \chi (D_\mu H)^\dagger D^\mu H \quad (2)$$

where  $D_\mu H$  is the ordinary covariant derivative acting on the SM Higgs doublet. Expanding out the covariant derivative and replacing  $H$  by its vacuum expectation value, we arrive at

$$\frac{m_W^2}{\Lambda_5^3} \bar{\chi} \chi W^{+\mu} W_\mu^- + \frac{m_Z^2}{2\Lambda_5^3} \bar{\chi} \chi Z^\mu Z_\mu. \quad (3)$$

It is worth noting that while the overall size of both couplings may be varied by shifting  $v^2/\Lambda_5^3$ , the ratio of the couplings to pairs of  $W$  and  $Z$  bosons are fixed with respect to one other. At higher order, this operator also results in couplings to pairs of photons and to  $Z\gamma$  through loops of  $W$  bosons.

At dimension 7, there are also couplings to the kinetic terms of the electroweak bosons,

$$L = \frac{1}{\Lambda_7^3} \bar{\chi} \chi \sum_i k_i F_i^{\mu\nu} F_{\mu\nu}^i \quad (4)$$

where  $F_i$ ,  $i = 1, 2, 3$  are the field strengths for the SM  $U(1)$ ,  $SU(2)$ , and  $SU(3)$  gauge groups. The couplings of dark matter to pairs of SM gauge bosons are given by:

$$g_{gg} = \frac{k_3}{\Lambda_7^3} \quad (5)$$

$$g_{WW} = \frac{2k_2}{s_w^2 \Lambda_7^3} \quad (6)$$

$$g_{ZZ} = \frac{1}{4s_w^2 \Lambda_7^3} \left( \frac{k_1 s_w^2}{c_w^2} + \frac{k_2 c_w^2}{s_w^2} \right) \quad (7)$$

$$g_{\gamma\gamma} = \frac{1}{4c_w^2} \frac{k_1 + k_2}{\Lambda_7^3} \quad (8)$$

$$g_{Z\gamma} = \frac{1}{2s_w c_w \Lambda_7^3} \left( \frac{k_2}{s_w^2} - \frac{k_1}{c_w^2} \right) \quad (9)$$

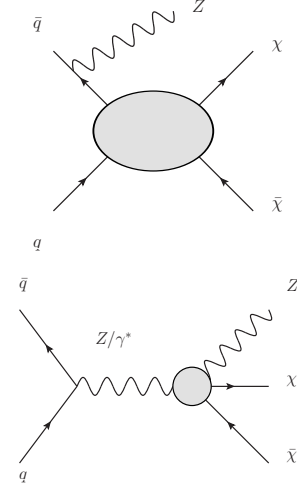


FIG. 1: Representative diagrams for production of dark matter pairs ( $\chi\bar{\chi}$ ) associated with a  $Z$  boson in theories where dark matter interacts with quarks (top) or directly with  $Z$  boson pairs (bottom).

TABLE I: Production cross sections (in fb) for pair production of WIMPs in association with a  $Z$  boson,  $pp \rightarrow Z\chi\bar{\chi} \rightarrow \ell^+\ell^-\chi\bar{\chi}$ , in theories where the dark matter interacts primarily with quarks, for  $\Lambda_i = 1$  TeV and  $\sqrt{s} = 7$  TeV.

$m_\chi$ (GeV)	D1	D5	D8	D9
	[ $\times 10^{-8}$ ]			
$\leq 10$	0.94	0.56	0.55	7.9
100	0.59	0.51	0.42	6.9
200	0.28	0.40	0.27	5.2
400	0.05	0.20	0.09	2.4
1000	$3 \times 10^{-4}$	0.01	0.002	0.1

where  $s_w$  and  $c_w$  are the sine and cosine of the weak mixing angle, respectively. For these kinetic operators, the over-all size can be thought of as controlled by  $k_2/\Lambda_7^3$ , but there is still freedom to adjust the relative importance of various pairs by adjusting  $k_1/k_2$ .

### DARK MATTER PRODUCTION IN ASSOCIATION WITH A $Z$ BOSON

The process of interest is pair-production of dark matter particles in conjunction with one  $Z$  boson. Representative Feynman diagrams are shown in Figure 1, for both the case of interactions with quarks as well as dark matter which interacts directly with weak bosons. In order to match on to the existing ATLAS  $ZZ$  measurement, we consider  $pp$  collisions at  $\sqrt{s} = 7$  TeV. Cross sections for each of the quark operators of Eq. (1) are presented for various dark matter masses and the corresponding  $\Lambda$  set equal to 1 TeV in Table I. These cross sections scale as  $\propto 1/\Lambda_{D1}^6$  for operator D1, and as  $\propto 1/\Lambda^4$  for D5, D8,

and D9. The rates for D1 are considerably smaller, due to suppression of the contribution of valence quark contributions by the small up and down quark masses. For this operator, loops involving the top quark are expected to be sizable and will result in an increase of the rate [24].

In part because of the rather stiff branching ratio penalty in asking for  $Z \rightarrow e^+e^-$  or  $\mu^+\mu^-$ , the rate for the operators describing interactions with quarks is somewhat smaller than the corresponding rates for mono-jets, mono-photons, or mono- $W$ s. However, the mono- $Z$  signature is nonetheless worth exploring, in part because it samples a different weighting of couplings to up-type versus down-type quarks, but also because the systematic uncertainties on the backgrounds should scale more favorably for mono- $Z$  than for mono-jets or even mono-photons, given that fake “QCD” backgrounds should be much smaller for mono- $Z$ s.

For the case of direct interactions with weak bosons, the dimension 5 operator is mediated only by  $Z$  exchange, whereas the dimension 7 operator contains a mixture of  $Z$  and photon exchange, with the relative importance of the two controlled by  $k_1/k_2$ . We consider two example admixtures of the dimension 7 operators:

- $k_1 = k_2$  leading to contributions from both  $Z$  and  $\gamma$  exchange.
- $k_1 = c_w^2/s_w^2 k_2$ , for which the  $\gamma$  exchange graph is negligible.

## ATLAS RESULTS

The ATLAS collaboration performed a measurement of the  $ZZ \rightarrow \ell\ell\nu\nu$  cross-section [8] in  $pp$  data with  $\sqrt{s} = 7$  TeV and integrated luminosity of  $4.6 \text{ fb}^{-1}$ . The fiducial region is defined as:

- two same-flavor opposite-sign electrons or muons, each with  $p_T^\ell > 20 \text{ GeV}$ ,  $|\eta^\ell| < 2.5$ ;
- dilepton invariant mass close to the  $Z$  boson mass:  $m_{\ell\ell} \in [76, 106] \text{ GeV}$ ;
- no particle-level jet with  $p_T^j > 25 \text{ GeV}$  and  $|\eta^j| < 4.5$ ;
- $(|p_T^{\nu\bar{\nu}} - p_T^Z|)/p_T^Z < 0.4$ ;
- $-p_T^{\nu\bar{\nu}} \times \cos(\Delta\phi(p_T^{\nu\bar{\nu}}, p_T^Z)) > 75 \text{ GeV}$ .

The results are consistent with Standard Model expectations (within  $1\sigma$  for the  $\mu^+\mu^-$  channel and within  $2\sigma$  over-all), as shown in Table II.

We use the expected background yield with uncertainties to calculate an upper limit on the number of events due to a new source which could be present in the collected data. Using the CLs method [25, 26], we find

TABLE II: Expected backgrounds and observed data in the ATLAS  $ZZ \rightarrow \ell\ell\nu\nu$  analysis [8] in  $pp$  collisions at  $\sqrt{s} = 7$  TeV with integrated luminosity of  $4.6 \text{ fb}^{-1}$ . The first uncertainty is statistical and systematic and the second uncertainty is luminosity.

	$ee\nu\nu$	$\mu\mu\nu\nu$	$\ell\ell\nu\nu$
Background	$20.8 \pm 2.7$	$26.1 \pm 3.3$	$46.9 \pm 5.5$
SM $ZZ \rightarrow \ell\ell\nu\nu$	$17.8 \pm 1.8$	$21.6 \pm 2.2$	$39.3 \pm 4.0$
Total	$38.6 \pm 3.8$	$47.7 \pm 4.6$	$86.2 \pm 7.2$
Data	35	52	87

$N < 18.0$  at 90% confidence limit (CL). We convert this to a limit on the cross section ( $\sigma$ ) for new physics based on  $N = \sigma \times \epsilon \times \mathcal{L}$ , where  $\epsilon$  is the fraction of new physics events which satisfy the selection requirements.

To aid the reinterpretation of the result, ATLAS has divided their calculation of  $\epsilon = A_{ZZ} \times C_{ZZ}$  into two pieces: the fiducial acceptance ( $A_{ZZ}$ ), the fraction of events which fall into a specified parton-level fiducial region, and the reconstruction efficiency ( $C_{ZZ}$ ), the fraction of events in the fiducial region which satisfy the final selection. We expect the reconstruction efficiency  $C_{ZZ}$  to be largely model independent, as the fiducial region is chosen such that  $C_{ZZ}$  is determined by the detector performance for specific final state objects rather than the production mechanism. Therefore, a calculation of the fiducial acceptance for a new model is all that is needed for an estimate of the total efficiency  $\epsilon$ . In terms of the fiducial acceptance  $A_{ZZ}$ , the limits are

$$\sigma < \frac{N}{A_{ZZ} \times C_{ZZ} \times \mathcal{L}}, \quad (10)$$

which results at the 90% CL in,

$$\sigma(90\% \text{ CL}) < \frac{18.0}{A_{ZZ} \times 0.679 \times 4.6 \text{ fb}^{-1}}. \quad (11)$$

## INTERPRETATION

We simulate the predicted  $Z\bar{\chi}\chi$  events for each of the EFTs described above, using MADGRAPH [27], with showering and hadronization provided by PYTHIA [28] and particle-level jet clustering with FASTJET [29]. We work at tree level, though it should be noted that very recently the next to leading order rates for several operators have been computed [30], and result in a modest increase in the expected rates. For each of the EFTs and a variety of dark matter masses, we compute the fiducial acceptance as defined above. The resulting acceptances for each EFT as a function of the dark matter mass are shown in Figure 2. The acceptance varies between about  $\approx 20 - 35\%$ , depending on the operator, and is roughly constant up to dark matter masses of about 1 TeV.

Combined with the ATLAS measurement, the acceptances translate into bounds on the production cross sec-

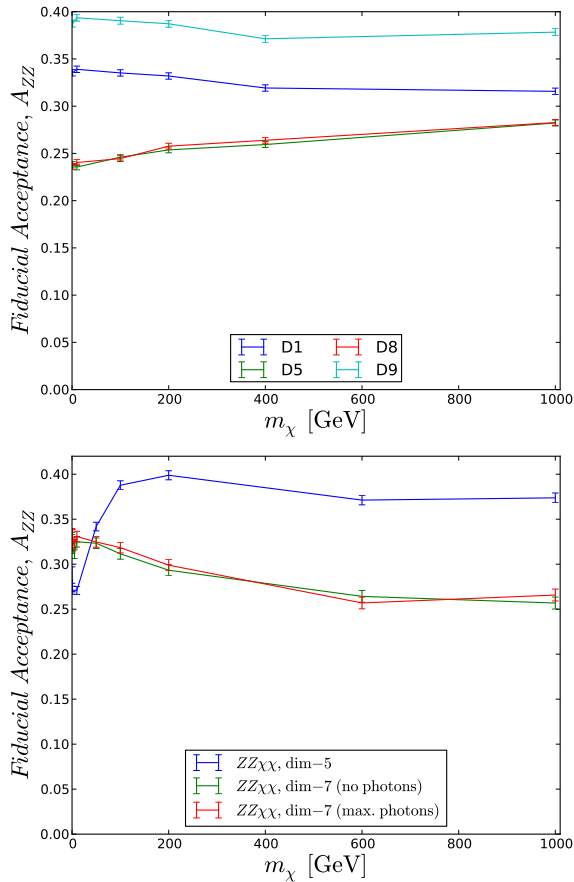


FIG. 2: Acceptance of the dark matter production process,  $pp \rightarrow Z\chi\bar{\chi}$ , with  $Z \rightarrow \ell^+\ell^-$ , for the ATLAS  $ZZ \rightarrow \ell\ell\nu\nu$  fiducial region (see text) as a function of the dark matter mass.

tion of  $\sigma(Z\chi\bar{\chi}) \lesssim 10 - 100$  fb at 90% CL. It is worth noting that the fiducial acceptance is significantly higher for dark matter production than for the SM  $ZZ$  production due to the larger missing transverse momentum in the  $Z\chi\bar{\chi}$ , as shown in Figure 3 for a sample parameter point with  $m_\chi = 100$  GeV and  $\Lambda = 1$  TeV. For each interaction type, we determine the lower bound on the scale  $\Lambda$  which characterizes its strength. The results are presented in Figure 4, which indicate that for some types of interactions, scales on the order of 100 GeV to TeV can be probed.

For the case of interactions with quarks, we further translate these bounds into the plane of spin-independent (SI) and spin-dependent (SD) scattering with nucleons, as related in [18]. These bounds are shown in Figure 5, along with bounds from CoGeNT [31] and Xenon 100 [32], and competing collider results from mono-jet and mono-photon searches. As is typical, bounds from colliders provide a unique probe of very light dark matter particles, and dominate as probes of spin-dependent interactions. Of course, the collider bounds are subject to the assumption that the EFT containing a contact inter-

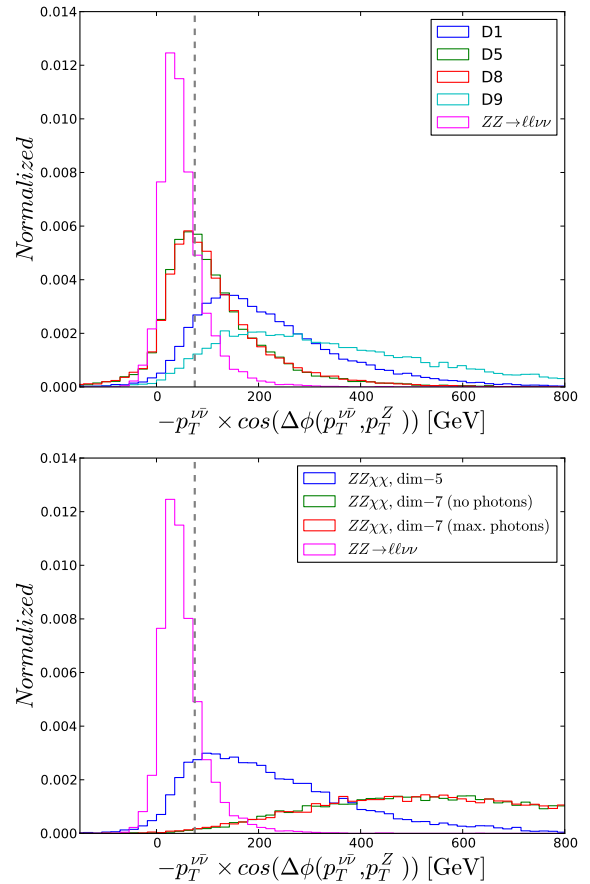


FIG. 3: Distribution of axial missing transverse momentum in simulated Standard Model  $ZZ \rightarrow \ell\ell\nu\nu$  and  $pp \rightarrow Z\chi\bar{\chi}$ , in the EFTs described in the text, for  $\Lambda = 1$  TeV and  $m_\chi = 100$  GeV at  $\sqrt{s} = 7$  TeV.

action is a good description of the physics. In cases with light mediating particles, these bounds can sometimes be weaker. Over-all, the two searches exhibit a high degree of complementarity.

## CONCLUSIONS

In this article, we have looked at the collider production of dark matter pairs in association with a  $Z$  boson which decays into charged leptons, a signature we refer to as a mono- $Z$ . We work in the context of effective field theories in which the dark matter either interacts directly with quarks, or with a pair of electroweak bosons. We derive limits on the strength of such interactions based on the recent ATLAS measurement of  $ZZ$  production (where one  $Z$  decays into charged leptons and the other into neutrinos) and find that the current limits already probe the TeV scale for some types of interactions.

For the case of interactions directly with quarks, the mono- $Z$  signature provides limits which are somewhat weaker than those from mono-jets or mono-photons.

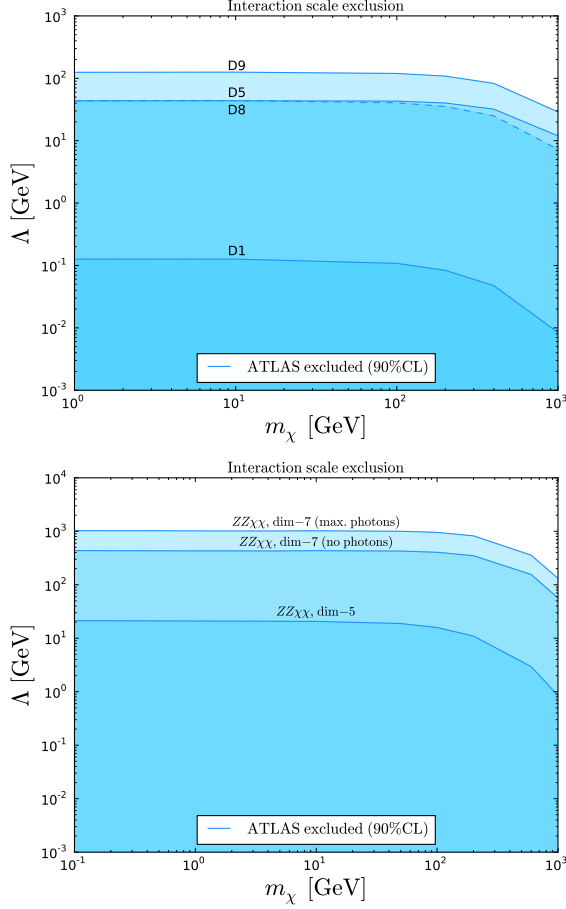


FIG. 4: Excluded region (blue) at 90% CL for the indicated interactions as a function of dark matter mass. The two regions for the dimension 7  $ZZ\bar{\chi}\chi$  correspond to the choices of  $k_1/k_2$  discussed in the text, with either maximal contribution from photon graphs (upper curve) or no contribution (lower curve).

Nonetheless, mono- $Z$  searches are expected to be less subject to systematic uncertainties from jet energy scales and photon identification, and thus may scale better at large luminosities. If a discovery is made, the mono- $Z$  signature offers a different way to dissect the couplings of up-type versus down-type quarks. If the dominant interaction is instead to pairs of weak bosons, colliders offer a unique opportunity for discovery.

Our results illustrate the complementarity between collider and direct searches of dark matter, and show how together they result in a more complete picture of dark matter interactions with the SM fields.

#### ACKNOWLEDGEMENTS

DW, CS and AN are supported by grants from the Department of Energy Office of Science and by the Alfred P. Sloan Foundation. TMPT is supported in part by NSF

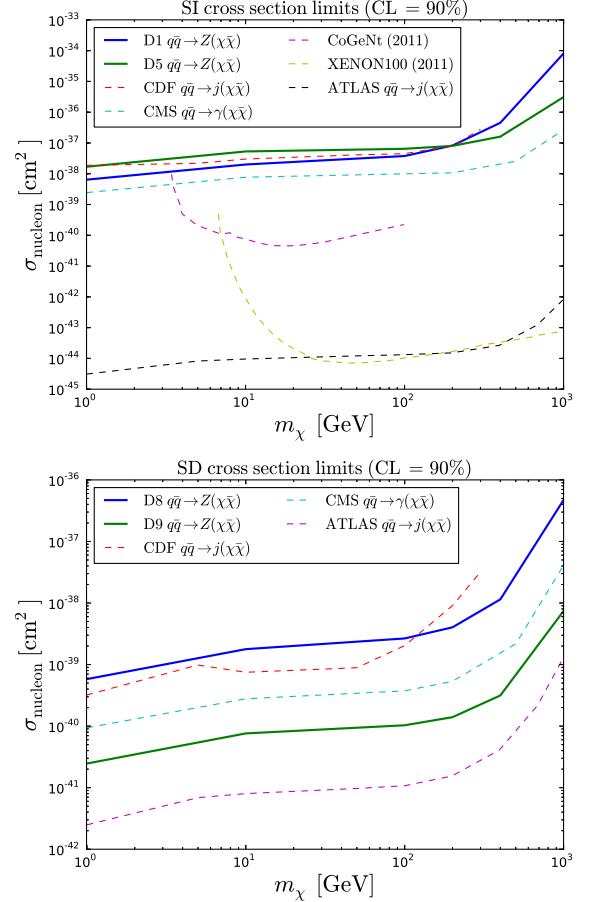


FIG. 5: Exclusion regions at 90% CL in the plane of the dark matter mass ( $m_\chi$ ) versus dark matter - nucleon spin-independent (top) or spin-dependent (bottom) cross-section plane. Results from this analysis are compared to existing collider and direct detection limits.

Grant PHY-0970171.

- 
- [1] D. E. Morrissey, T. Plehn and T. M. P. Tait, Phys. Rept. **515**, 1 (2012) [arXiv:0912.3259 [hep-ph]].
  - [2] CDF Collaboration, Phys. Rev. Lett. **108**, 211804 (2012).
  - [3] G. Aad *et al.* [ATLAS Collaboration], arXiv:1210.4491 [hep-ex].
  - [4] S. Chatrchyan *et al.* [CMS Collaboration], JHEP **1209**, 094 (2012) [arXiv:1206.5663 [hep-ex]].
  - [5] G. Aad *et al.* [ATLAS Collaboration], arXiv:1209.4625 [hep-ex].
  - [6] S. Chatrchyan *et al.* [CMS Collaboration], Phys. Rev. Lett. **108**, 261803 (2012) [arXiv:1204.0821 [hep-ex]].
  - [7] Y. Bai and T. M. P. Tait, arXiv:1208.4361 [hep-ph].
  - [8] G. Aad *et al.* [ATLAS Collaboration], arXiv:1211.6096 [hep-ex] (2012).
  - [9] F. J. Petriello, S. Quackenbush, K. M. Zurek, arXiv:0803.4005v2 [hep-ph].
  - [10] N. F. Bell, J. B. Dent, A. J. Galea, T. D. Jacques,

- L. M. Krauss and T. J. Weiler, arXiv:1209.0231 [hep-ph].
- [11] M. T. Frandsen, U. Haisch, F. Kahlhoefer, P. Mertsch and K. Schmidt-Hoberg, JCAP **1210**, 033 (2012) [arXiv:1207.3971 [hep-ph]].
  - [12] M. Beltran, D. Hooper, E. W. Kolb and Z. C. Krusberg, Phys. Rev. D **80**, 043509 (2009) [arXiv:0808.3384 [hep-ph]].
  - [13] W. Shepherd, T. M. P. Tait and G. Zaharijas, Phys. Rev. D **79**, 055022 (2009) [arXiv:0901.2125 [hep-ph]].
  - [14] Q. -H. Cao, C. -R. Chen, C. S. Li and H. Zhang, JHEP **1108**, 018 (2011) [arXiv:0912.4511 [hep-ph]].
  - [15] M. Beltran, D. Hooper, E. W. Kolb, Z. A. C. Krusberg and T. M. P. Tait, JHEP **1009**, 037 (2010) [arXiv:1002.4137 [hep-ph]].
  - [16] J. Goodman, M. Ibe, A. Rajaraman, W. Shepherd, T. M. P. Tait and H. -B. Yu, Phys. Lett. B **695**, 185 (2011) [arXiv:1005.1286 [hep-ph]].
  - [17] Y. Bai, P. J. Fox and R. Harnik, JHEP **1012**, 048 (2010) [arXiv:1005.3797 [hep-ph]].
  - [18] J. Goodman, M. Ibe, A. Rajaraman, W. Shepherd, T. M. P. Tait and H. -B. Yu, Phys. Rev. D **82**, 116010 (2010) [arXiv:1008.1783 [hep-ph]].
  - [19] A. Rajaraman, W. Shepherd, T. M. P. Tait and A. M. Wijangco, Phys. Rev. D **84**, 095013 (2011) [arXiv:1108.1196 [hep-ph]].
  - [20] P. J. Fox, R. Harnik, J. Kopp and Y. Tsai, Phys. Rev. D **85**, 056011 (2012) [arXiv:1109.4398 [hep-ph]].
  - [21] K. Cheung, P. -Y. Tseng, Y. -L. S. Tsai and T. -C. Yuan, JCAP **1205**, 001 (2012) [arXiv:1201.3402 [hep-ph]].
  - [22] A. Rajaraman, T. M. P. Tait and D. Whiteson, JCAP **1209**, 003 (2012) [arXiv:1205.4723 [hep-ph]].
  - [23] R. C. Cotta, J. L. Hewett, M. P. Le and T. G. Rizzo, arXiv:1210.0525 [hep-ph].
  - [24] U. Haisch, F. Kahlhoefer and J. Unwin, arXiv:1208.4605 [hep-ph].
  - [25] A. Read, J. Phys. G: Nucl. Part. Phys. **28**, 2693 (2002);
  - [26] T. Junk, Nucl. Instrum. Methods A **434**, 425 (1999).
  - [27] J. Alwall, M. Herquet, F. Maltoni, O. Mattelaer and T. Stelzer, JHEP **1106**, 128 (2011) [arXiv:1106.0522 [hep-ph]].
  - [28] T. Sjostrand, S. Mrenna and P. Z. Skands, JHEP **0605**, 026 (2006) [hep-ph/0603175].
  - [29] M. Cacciari, G.P. Salam and G. Soyez, arXiv:1111.6097 (2011).
  - [30] P. J. Fox and C. Williams, arXiv:1211.6390 [hep-ph].
  - [31] C. E. Aalseth *et al.* [CoGeNT Collaboration], Phys. Rev. Lett. **106**, 131301 (2011) [arXiv:1002.4703 [astro-ph.CO]].
  - [32] E. Aprile *et al.* [XENON100 Collaboration], Phys. Rev. Lett. **109**, 181301 (2012) [arXiv:1207.5988 [astro-ph.CO]].